

Article

Not peer-reviewed version

# Toxicity Evaluation and Control Release of Curcumin-Loaded Amphiphilic Poly-n-vinylpyrrolidone Nanoparticles for the Treatment of Malignant Tumors: In Vitro and In Vivo Models

[Anna L. Luss](#)\*, [Dmitry V. Bagrov](#), [Anne V. Yagolovich](#), Ekaterina V. Kukovyakina, Irina I. Khan, Vadim S. Pokrovsky, [Maria V. Shestovskaya](#), [Marine E. Gasparian](#), [Dmitry A. Dolgikh](#), [Andrey N. Kuskov](#)

Posted Date: 15 December 2023

doi: 10.20944/preprints202312.1140.v1

Keywords: curcumin; poly-n-vinylpyrrolidone; nanoparticles; micelles; glioblastoma; toxicity



Preprints.org is a free multidiscipline platform providing preprint service that is dedicated to making early versions of research outputs permanently available and citable. Preprints posted at Preprints.org appear in Web of Science, Crossref, Google Scholar, Scilit, Europe PMC.

Copyright: This is an open access article distributed under the Creative Commons Attribution License which permits unrestricted use, distribution, and reproduction in any medium, provided the original work is properly cited.

## Article

# Toxicity Evaluation and Control Release of Curcumin-Loaded Amphiphilic Poly-N-Vinylpyrrolidone Nanoparticles: In Vitro and In Vivo Models

Anna L. Luss <sup>1,\*</sup>, Dmitry V. Bagrov <sup>2</sup>, Anne V. Yagolovich <sup>2,3</sup>, Ekaterina V. Kukovyakina <sup>1</sup>, Irina I. Khan <sup>4,5</sup>, Vadim S. Pokrovsky <sup>4,5</sup>, Maria V. Shestovskaya <sup>1</sup>, Marine E. Gasparian <sup>1,3</sup>, Dmitry A. Dolgikh <sup>2,3</sup> and Andrey N. Kuskov <sup>1</sup>

<sup>1</sup> Department of Technology of Chemical, Pharmaceutical and Cosmetic Products, D. Mendeleev University of Chemical Technology of Russia, 125047 Moscow, Russia

<sup>2</sup> Faculty of Biology, Lomonosov Moscow State University, 119234 Moscow, Russia

<sup>3</sup> Shemyakin-Ovchinnikov Institute of Bioorganic Chemistry of the Russian Academy of Sciences, 117997 Moscow, Russia

<sup>4</sup> N.N. Blokhin National Medical Research Center of Oncology, Ministry of Health of Russia, 115478 Moscow, Russia

<sup>5</sup> People's Friendship University of Russia (RUDN University), Moscow, 117198, Russia

\* Correspondence: al.luss@yandex.ru;

**Abstract:** Curcumin attracts a huge attention because of its biological properties: antiproliferative, antioxidant, anti-inflammatory, immunomodulatory and so on. However, its usage has been limited by poor water solubility and low bioavailability. Herein, to solve these problems we developed curcumin-loaded nanoparticles based on end-capped amphiphilic poly(N-vinylpyrrolidone). Nanoparticles were obtained using the solvent evaporation method and were characterized by dynamic and electrophoretic light scattering, transmission electron microscopy and atomic force microscopy. The average particle size was 200 nm, and  $\zeta$ -potential was -4 mV. Curcumin release studies showed that nanoparticles are stable in aqueous solution. In vitro release study showed prolonged action in gastric, intestinal and colonic fluids, consistently and in PBS. In vitro studies on epidermoid carcinoma and human embryonic kidney cells showed that the cells absorbed more curcumin in nanoparticles compared to free curcumin. Nanoparticles are safe for healthy cells and show high cytotoxicity for glioblastoma cells in cytotoxicity studies *in vitro*. Median lethal dose was determined in acute toxicity assay on Zebrafish and was 23  $\mu$ M. Overall, the curcumin-loaded nanoparticles seem promising for cancer treatment.

**Keywords:** Curcumin; poly-N-vinylpyrrolidone; nanoparticles; glioblastoma; toxicity

## 1. Introduction

In recent years, micelles have been studied as one of the most promising strategies for site-specific drug delivery. One of the most well-known polymers for creating micellar delivery systems is polyethylene glycol (PEG) [1–3]. Despite the well-studied chemistry of PEG, there is currently an active search for alternative polymers/copolymers for the delivery of physiologically active substances with similar properties. Polylactide [4,5], poly-lactide-co-glycolide [6–8], poly- $\epsilon$ -caprolactone [9,10] and others are also used as carriers.

In the last decade, interest has arisen in carriers based on poly-N-vinylpyrrolidone (PVP) [11,12]. Like PEG, PVP has a very long history of medical use [13,14]. From a pharmaceutical point of view, it has attracted significant interest due to certain physico-chemical properties: solubility in almost all solvents, affinity for hydrophobic and hydrophilic surfaces, ability to form complexes, superior bioavailability, biocompatibility [13]. PVP is widely used in medicine as an antiseptic in combination with iodine and as a component of solutions for contact lenses [15,16]. Moreover, it is included in the

FDA's database of inactive ingredients for use in oral, topical and injectable pharmaceutical products [17].

Amphiphilic PVP derivatives with hydrophobic terminal groups have been studied over the past decades as intravenous drug delivery systems [18–20]. They self-organize in aqueous solutions to form micellar structures and demonstrate excellent hemo- and biocompatibility. Compared to standard nanoparticles (PLGA, PLA, etc.), such aggregates have a hydrophilic outer shell and inner hydrophobic core, which allows the encapsulation of hydrophobic substances with high efficiency. Parameters such as copolymer molecular weight, morphology and size of micelles are easily controlled during the synthesis process. They can capture various therapeutic agents, such as non-steroidal anti-inflammatory drugs [19–21], antitumor drugs [22], antifungal antibiotics [23], cytokines [24,25] and plasmid DNA [26] into micelles. Depending on the average hydrodynamic radius, nanoparticles can be absorbed by cell cultures through various mechanisms, including endocytosis and membrane fusion, which allows selective delivery of the active substance to both cell endosomes and its nucleus [27]. In addition, PVP nanoparticles can be used as effective modifiers of liposomal membranes, increasing their stability [23].

Curcumin is a natural polyphenol found in turmeric. Its clinical potential is determined by anti-inflammatory [28], antimicrobial [29], anti-carcinogenic [30,31], hypoglycemic [32,33] and immunomodulating [34] and other properties. Curcumin has a very promising property, namely increased uptake by tumor cells *in vitro*. Moreover, its pro-apoptotic effect increases with increasing intracellular concentration, which may be promising in the development of drugs against malignant neoplasms, including glioblastoma and colorectal cancer [35–39]. Curcumin has also been shown to be effective not only as an anticancer drug, but also in the fields of oral hygiene, periodontal therapy, gastrointestinal diseases, ophthalmic drugs and wound healing [37]. Despite its wide range of biological activities, curcumin has low bioavailability due to its poor solubility in aqueous media and low stability in the presence of air and UV-radiation [40,41]. These limitations represent a major problem to the study and application of curcumin in biomedicine. A solution to this problem could be the effective encapsulation of curcumin into nanoparticles [42].

Herein, we report the preparation of curcumin-loaded nanoparticles based on amphiphilic PVP end-capped with tioctadecyl group. PVP with a molecular weight of 6 kDa was selected based on previous studies as the most suitable candidate to achieve maximum encapsulation of curcumin by its lipophilic lyophobic balance. Nanoparticles were prepared by solvent evaporation method. Anticancer activity of curcumin-loaded PVP was estimated in glioblastoma cell lines. In addition, *in vitro* release dynamics were measured in various environments, and the acute toxicity of zebrafish *in vivo* was noted.

## 2. Materials and Methods

### 2.1. Materials

N-vinylpyrrolidone, octadecyl mercaptan (ODM) were obtained from Sigma-Aldrich (St. Louis, USA). Azobisisobutyronitrile (AIBN) was obtained from Chemical Line (St. Petersburg, Russia). 1,4-dioxane was obtained from LenReaktiv (St. Petersburg, Russia). Curcumin was obtained from MT BIO-TECH (Hunan, China). All chemicals were used without further purification unless otherwise stated. All solvents and components of buffer solutions were used as received.

### 2.2. Synthesis and physicochemical characteristics of nanoparticles based on amphiphilic poly(N-vinylpyrrolidone)

#### 2.2.1. Synthesis of amphiphilic poly(N-vinylpyrrolidone)

The synthesis of amphiphilic poly(N-vinylpyrrolidone) with a molecular weight of 6 kDa was carried out in accordance with [18,27,43]. Briefly, 20 ml of N-vinylpyrrolidone, AIBN 1 wt% (0.7 mol%) and ODM 0.25 wt% (1 mol%) were dissolved in 40 ml of 1,4-dioxane. The reaction was carried out at 70°C for 3 hours. The resulting solution was dialyzed against water, frozen and freeze-dried.

Molecular weight was determined by reverse iodometric titration according to the method [44] and it was 6 kDa. The absence of solvent residues was determined by thermogravimetric analysis.

#### 2.2.2. Synthesis of curcumin-loaded nanoparticles based on amphiphilic poly(N-vinylpyrrolidone)

A 90 mg sample of amphiphilic poly(N-vinylpyrrolidone) was dissolved in 30 ml of water (3 mg/ml). 4 ml of curcumin solution in acetone (2.5 mg/ml) was added to the resulting solution. Then the resulting mixture was dispersed on an ultrasonic homogenizer Bandelin SONOPULS HD 4400 (Berlin, Germany) in the 1s on 1 s off mode and an amplitude of 25% for 20 minutes. Then the solvent was distilled off using a Heidolph Hei-VAP Ultimate rotary evaporator (Schwabach, Germany), and the resulting suspension of nanoparticles (PVP-Cur NPs) was centrifuged at 4000 rpm. Supernatant was frozen and freeze-dried.

#### 2.2.3. Determination of particle size and surface charge

The  $\zeta$ - potential and hydrodynamic diameter of the nanoparticles were determined using a Malvern Zetasizer Nano Z&S (Worcestershire, UK). Measurements were carried out at 25°C and in distilled water three times for each sample.

#### 2.2.4. Transmission electron microscopy and atomic-force microscopy

The PVP-Cur NPs were visualized using transmission electron microscopy (TEM) and atomic-force microscopy (AFM). For the both imaging procedures, the NPs were deposited onto carbon-formvar TEM grids (mesh 200, EMS, USA). The grids were treated using a glow discharge device K100X (Emitech, currently Quorum Technologies, Lewis, UK) at 30 mA for 30 s. For the TEM imaging, the sample was diluted in water to  $c=0.1$  mg/mL, deposited onto the grids for approximately 1 minute, then the grids were stained by 1% uranyl acetate and dried. Images were carried out using a JEM-1400 electron microscope (JEOL, Japan) operating at 120 kV, equipped with Rio-9 camera (Gatan Inc., USA).

For the AFM imaging, the sample was diluted in water to  $c=0.25$  mg/mL, deposited onto the grids for approximately 1 minute, then the grids were washed with water and dried. The images were acquired in semicontact mode, using a Solver PRO-M microscope (NT-MDT, Zelenograd, Russia). The scanning rate was 1-1.7 Hz, the NSG10 cantilevers (Tips-Nano, Russia) were used (typical curvature radius 6 nm, typical force constant  $k=11.8$  N/m).

Image processing was carried out using Fiji [45] and FemtoScan Online [46] for the TEM images and AFM frames, respectively.

#### 2.2.5. Evaluation of curcumin encapsulation in the PVP-Cur NPs

The curcumin encapsulation efficiency was calculated by ratio of total curcumin content in PVP-Cur NPs to total drug amount according to [47]. The percent of loaded drug was calculated from the total amount of drug extracted from the PVP-Cur NPs to the known weight of nanoparticles. To extract curcumin, lyophilized PVP-Cur NPs were dissolved in acetonitrile (5 mg in 5 ml). The samples were stirred at 500 rpm for 2 hours for full curcumin extraction. Then the samples were centrifuged at 10,000 rpm and supernatants were collected. Suspension (20  $\mu$ l) was dissolved in ethanol (1 ml) and used for the further estimations. The curcumin concentrations were measured spectrophotometrically at 425 nm.

Curcumin loading efficiency (LE) was calculated using following equation:

$$LE(\%) = \frac{\text{Total curcumin content in NPs}}{\text{Total curcumin amount}} \times 100\%$$

Curcumin loading capacity (LC) in the preparations was calculated using following equation:

$$LC(\%) = \frac{\text{Curcumin content}}{\text{Weight of nanoparticles}} \times 100\%$$

### 2.3. Curcumin in vitro release study

### 2.3.1. Curcumin release in PBS Solution

Curcumin *in vitro* release profile from the PVP-Cur NPs was obtained using dialysis technique as described [48]. PVP-Cur NPs were resuspended in 5ml of PBS (pH 7.4) and dialyzed using Thermo Fisher Scientific (USA) tubes with a molecular weight cut-off (MWCO) of 1000 Da. During dialysis, the tubes were placed in a glass with 150 ml of PBS and incubated at 37°C under constant shaking. The amount of curcumin released from PVP-Cur NPs was estimated by taking out 1.0 ml of buffer media at predetermined time intervals (0.5, 1, 2, 3, 4, 6, 8, 10, 12, 16, 20, 24, 36, 48 hours). The content of the released curcumin in selected samples was determined by spectrophotometry at 425 nm. Free curcumin dissolved in methanol/water mixture at the same amount as in PVP-Cur NPs was used as a control. All samples' measurements were run in triplicates. The standard curcumin calibration curve was obtained and used as a reference in the experiments.

### 2.3.2. *In vitro* curcumin release in simulated gastric, intestinal and colonic digestion

*In vitro* curcumin release from PVP-Cur NPs was estimated as described [49] using Simulated Gastric Fluid (SGF, pH=1.2) without enzymes (0.2% Polysorbate 80) for 2 hours, Simulated Intestinal Fluid (SIF, pH=6.8) without enzymes (0.2% Polysorbate 80) for 6 hours and Simulated Colonic Fluid (SCF, pH=7.4) (0.2% Polysorbate 80) with  $\beta$ -Galactosidase (0.13 units/ml) for 24 hours, at constant shaking and at 37°C. Release medium was centrifuged, and the absorbance was measured spectrophotometrically at 425 nm to determine the amount of the released curcumin. All samples' measurements were run in triplicates.

### 2.3.3. Stability studies

Stability characteristics of PVP-Cur NPs were evaluated according to the International Council for Harmonisation of Technical Requirements for Pharmaceuticals for Human Use (ICH) guidelines (2003) code Q1A(R2) (stability testing of new drug substances and products). Nanoparticles samples were stored preserved from light in closed impenetrable tubes. For the accelerated condition experiment, samples were taken at 0, 1, 2, 4 and 6 months (40 °C  $\pm$  2 °C, 75% relative humidity  $\pm$  5%). The amount of curcumin released from the samples was measured using UV-Vis spectrophotometer at 425 nm.

### 2.3.4. Water resuspendability study

Freeze-dried PVP-Cur NPs samples (10 mg) were dispersed in 10 ml of distilled water) and stirred for 5 minutes to test the homogeneity of the obtained suspensions using Zetasizer Nano Z&S (Malvern Instruments, UK).

## 2.4. *In vitro* and *in vivo* assays

### 2.4.1. Cell lines

A431 epidermoid carcinoma cells (ATCC no.CRL-1555<sup>TM</sup>) were cultured in DMEM with 4 mM L-glutamine supplemented with 10% FBS. Human embryonic kidney cells HEK 293 (ATCC no. CRL-1573<sup>TM</sup>) were cultured in Eagle's Minimum Essential Medium, and human glioblastoma cell lines T98G (ATCC no. CRL-1690<sup>TM</sup>) and U87 (ATCC no. HTB-14<sup>TM</sup>) were cultivated in Dulbecco's Modified Eagle Medium with 2 mM glutamine supplemented with 10% FBS. Cells were cultured at 37°C in 5% CO<sub>2</sub> in a humidified atmosphere. All cells were passaged with 0.25% v/w trypsin - 0.53 mM EDTA at 80% confluence.

Mouse embryonic fibroblasts NIH/3T3 cells (ATCC) were chosen as a control healthy cell line. NIH/3T3 were cultured in DMEM medium supplemented with 10% FBS, L-glutamine (1 mM) and penicillin-streptomycin (100 U/mL). Cells were incubated at 37 °C in a humidified atmosphere containing 5% CO<sub>2</sub> and split every 3 days using EDTA solution.

### 2.4.2. Cytotoxicity assay



The three cell lines (NIH/3T3, T98G and U87) were used in the cytotoxicity assay.

Viability of cells was estimated by measuring activity of mitochondrial NAD(P)H-dependent cellular oxidoreductase enzymes which could reduce a yellow tetrazolium salt (3-(4,5-dimethyl-2-thiazolyl)-2,5-diphenyl-2-H-tetrazolium bromide), or MTT) to a violet formazan dye by metabolically active cells.

Cells were seeded in a 96-well plate in the amount of  $8 \times 10^3$  cells per well. After overnight incubation, the studied substances (PVP, Curcumin, PVP-Cur NPs) were added to cells in various concentrations in 100  $\mu$ l of culture medium. After 24h of drug exposition, cells were treated with 20  $\mu$ l of MTT solution (MTT Cell Viability Assay Kit, Servicebio). In parallel, MTT was added to the wells with DMEM medium with nanoparticles w/o cells, that were used further for optical compensation. Incubation with MTT lasted for 4 hours, then the medium was aspirated from the wells, and formazan crystals were dissolved in DMSO. The compensation for DMSO absorbance was also performed. Optical density was measured at 570 nm on a Tecan Infinite Infinite® M Nano + spectrophotometer. Absorption values were converted to percentages relative to absorption values of intact cells.

#### 2.4.3. Cell uptake assay

Cell uptake assay was studied on A431 and HEK 293 cell lines according to our previous works [27]. Briefly, the cells were seeded in a 96-well polystyrene plate at a density of  $5 \times 10^3$  cells per well. After 24 hours, the cells were washed with PBS and then preincubated for 15 min with Hoechst 33258 dissolved in the cell medium at a ratio of 1:1000, and then washed with the medium. After that, 150  $\mu$ l of DMEM supplemented with either free curcumin or with the PVP-Cur NPs was added to the wells. To analyze the distribution of curcumin, the cells were washed three times with PBS and then visualized using a Zeiss Axio Observer.Z1 inverted microscope (Carl Zeiss AG, Germany).

#### 2.4.4. Fish Embryo Acute Toxicity Test (FET)

Studies were conducted on Zebrafish (*Danio rerio*) in accordance with OECD guideline Protocol 236 "Fish Embryo Acute Toxicity (FET) Test" (OECD/OCDE, 2013). Morphological effects were assessed according to [50].

Adult wild-type zebrafish were kept in aquariums with an aeration and recirculation system at a temperature of 28°C, pH 6.5–7.5 with a photoperiod cycle of 14:10 h (light: dark). The fish were fed twice daily according to conventional recommendations (using zebrafish food).

Freshly laid eggs after fertilization (less 1-hour post-fertilization (hpf)) were collected and placed in *Danio rerio* E3 embryo water (5 mM NaCl, 0.33 mM CaCl<sub>2</sub>, 0.33 mM MgSO<sub>4</sub>·7H<sub>2</sub>O and 0.17 mM KCl and 0.1% methylene blue). Unfertilized eggs and embryos 24 hours after fertilization that had significant developmental defects were detected under a Nexcope NSZ-810 microscope (China) and removed from the experiment. Experimental embryos were mechanically dechorionized with tweezers and placed in 24-well plates (2 embryos per well, total 0.5–1.5 ml of solution per well). PVP-Cur NPs nanoparticles were added in quantities such that final concentrations ranged from 0.1–100  $\mu$ M of curcumin in each well. Each well was performed in triplicate (n=6 per group).

The embryos were examined 24 (48 hpf) and 72 (96 hpf) hours after the addition of nanoparticles; developmental disorders and delays, morphological changes, including irregular shape of the yolk sacs, impaired tail development, and decreased motor activity were recorded.

To estimate the full range of mortality from 0 to 100%, embryonic deaths were recorded at 24 (48 hpf) and 72 (96 hpf) hours after addition of compounds. Toxicity assay (LC<sub>50</sub> calculation) was determined based on cumulative mortality at the end of the experiment and was estimated using regression analysis.

#### 2.5. Statistical analysis

In cytotoxicity studies, the obtained data represented normal distribution. The experiments were performed for no less than three times in three replicates. Statistical analysis was held using ordinary

one-way ANOVA followed by Dunnett’s multiple comparisons test using Graphpad Prism 6.01 software (San Diego, CA, USA).

3. Results

3.1. Physicochemical characteristics of PVP-Cur NPS

The basic properties, size, shape and ζ-potential of the PVP-Cur NPs were determined after resuspension of the resulting samples in water. Water resuspendability test showed that freeze-dried PVP-Cur NPs samples were easily dispersed back in distilled water and appeared translucent similar to original nanoparticles dispersion before freeze-drying which was confirmed by the results of the dynamic light scattering (DLS) analysis. All basic properties are shown in Table 1.

Table 1. The main characteristics of the nanoparticles before and after freeze-drying.

PVP-Cur NPs	Z-average hydrodynamic diameter (nm ± SD)	LC (% mass ± SD)	LE (%mass ± SD)	ζ-potential (mV ± SD)
Before freeze-drying	191.1 ± 11,3	9.3 ± 0.3	93.9 ± 1.2	-4.00 ± 0,41
After freeze-drying	190.0 ±12,2	9.2 ± 0.5	93.6 ± 1.1	-4.21 ± 0.15

Given that the loading of curcumin was about 10% wt. of the polymer mass, the degree of encapsulation of biologically active substances in nanoparticles reached 95%.

The PVP-Cur NPs were spherical particles, as shown by transmission electron microscopy (TEM) (Figure 1 A,B) and atomic-force microscopy (AFM) (Figure 1C). For the AFM imaging, NPs were deposited onto TEM grids (amorphous carbon) rather than mica or graphite, which are commonly used as substrates. We chose the grids treated with the glow discharge, because the adsorption of the NPs onto their surface was relatively high, and they were previously used as substrates for the AFM imaging [51].

The size of the NPs was measured using TEM, AFM and DLS, and the obtained data are summarized in Figure 1 E.

The z-average size and the number average measured using DLS (190 nm and 150 nm, respectively (Figure 1 D,E) were higher than the mean particle size determined using microscopy. This is the difference between the particle hydrodynamic diameter measured by DLS and the particle projection diameter assessed by the AFM and TEM. A similar difference was observed for the poly(styrene-co-acrylic acid) copolymer particles [52]. The mean polydispersity index (PDI) of the NPs was 0.10±0.03 by DLS, which confirms the homogeneity of the analyzed NPs. The PDI based on the TEM data can be easily calculated by formula:

$$PDI = (\frac{SD}{mean\ diameter})^2$$

where SD – standard deviation.

In our case, according to the TEM data, SD=40 nm, mean diameter=118 nm, so we get an estimate for PDI~0.11, which is in agreement with the value obtained using DLS.

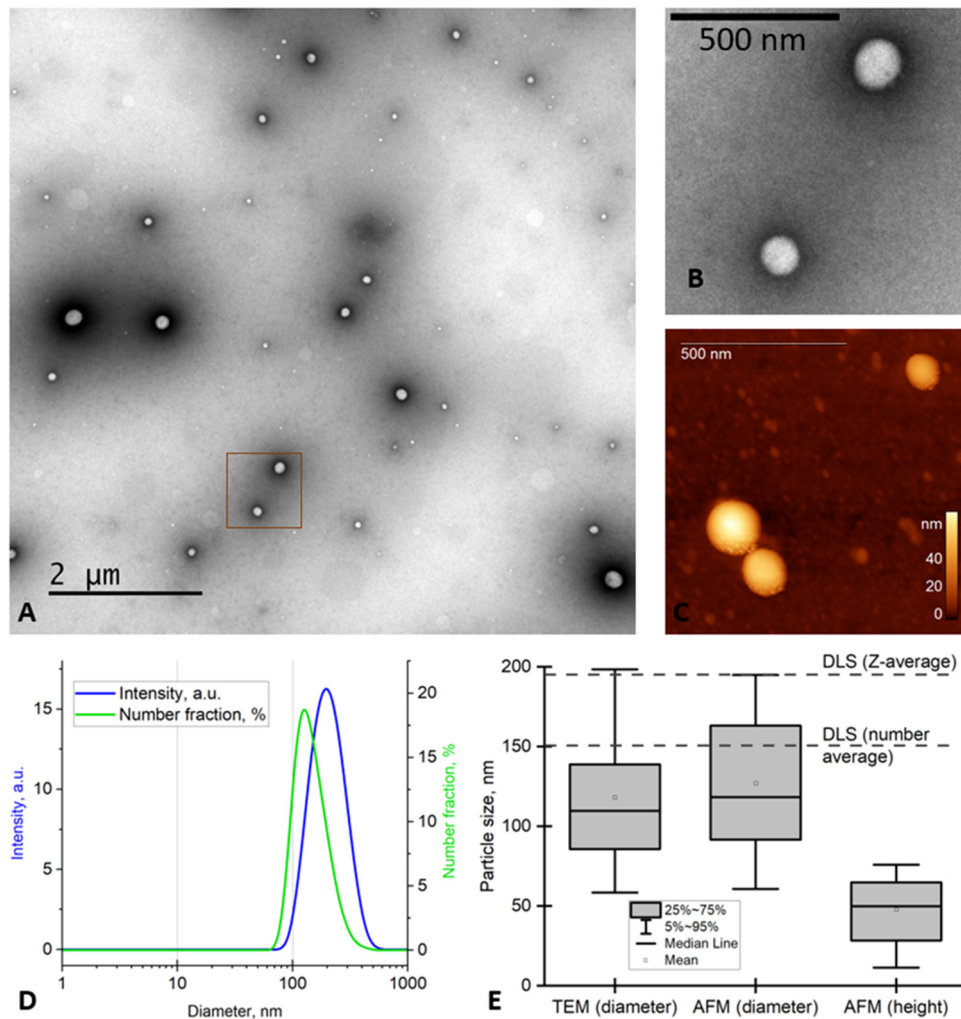


**Figure 1.** Characterization of the Amph-PVP-Cur NPs using TEM (A, B), AFM (C) and DLS (D), and the measured sizes (E). The image B shows the magnified part of the image A. The dotted lines in E show the z-average and the number average obtained using DLS.

Overall, the data obtained using the single-particle measurements (AFM, TEM) and ensemble measurements (DLS) were in good agreement.

### 3.2. Curcumin *in vitro* release study

PVP-Cur NPs were incubated at 37°C in PBS; the *in vitro* release profile studied over 48 hours is presented as a cumulative release percentage in Figure 2A.

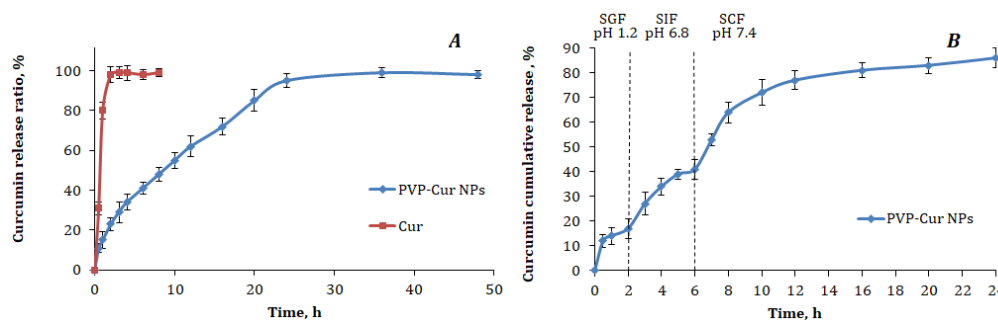


**Figure 2.** A - Curcumin *in vitro* release profiles from curcumin-loaded polymeric nanoparticles (PVP-Cur NPs) and curcumin solution (Cur) in PBS (pH 7.4) at 37°C; B - Cumulative curcumin release from



the PVP-Cur NPs into simulated gastric fluids modeling three digestive system tracts. Data are plotted as the average  $\pm$  SD of three measurements.

As one can see, a typical two-phase release profile was observed for the tested formulation when it was placed to the released medium. First, there was a relatively rapid release of about 10% of the loaded curcumin in the initial 30 minutes, followed by sustained release of the remained curcumin by 24 h. In comparison, over 30% of the curcumin from the control water/methanol mixture was released into the medium rapidly by 30 minutes, with further almost complete curcumin recovery after 3 hours.

The in vitro curcumin release study has been designed to simulate the human digestion tracks. The resulted curve of cumulative curcumin release from PVP-Cur NPs is presented in Figure 2B.

In the first medium, which simulated gastric fluid (pH 1.2) similar to the abovementioned experiment, there was observed a slight burst effect, which can be explained mostly by the release of curcumin bounded to the PVP outer shell . With the increase of pH value of the media in simulated intestinal fluid (pH 6.8) and simulated colonic fluid (pH 7.4), higher curcumin amounts were released in sustainable manner. The steps after 2 hours and 6 hours of the experiment were caused by the switch of the release media. The cumulative drug release for 24 hours from the PVP-Cur NPs was about 85%. It can also be mentioned that only rather small amount of curcumin was released to the fluid modeling the stomach acidic environment, while the highest amount of curcumin was released into the simulated colonic fluid.

During the stability test, no changes were observed in the content of curcumin in PVP-Cur NPs, as well as in their average size in accelerated stability studies (Table 2), which is the evidence of rather good stability of the obtained PVP-Cur NPs.

**Table 2.** Accelerated stability studies of PVP-Cur NPs according to the ICH guidelines.

Time (month)	Residual curcumin content (%)	Average size (nm $\pm$ SD)
0	100.00	190.0 $\pm$ 12.3
1	99.04	191.2 $\pm$ 13.3
2	97.23	189.5 $\pm$ 12.8
4	96.62	190.4 $\pm$ 12.9
6	94.11	190.3 $\pm$ 13.7

3.3. Cytotoxicity assay

The cytotoxicity of PVP-Cur NPs in comparison with Curcumin and PVP was studied in glioblastoma cell lines T98G and U87 (Figure 3A,B). Normal NIH/3T3 mouse embryonic fibroblasts were used as control (Figure 3C). The viability of fibroblast cells exceeded 85% for free curcumin and PVP-Cur. Viability was above 85% for free PVP. The half-maximal inhibition concentration (IC<sub>50</sub>) of curcumin was 70.1 $\pm$ 3.5  $\mu$ M for T98G cells and 48.6 $\pm$ 1.7  $\mu$ M for U87 cells. The IC<sub>50</sub> of PVP-Cur NPs was determined to be 29.3 $\pm$ 3.7  $\mu$ M and 20.7 $\pm$ 1.3  $\mu$ M for T98G and U87 cells, respectively.

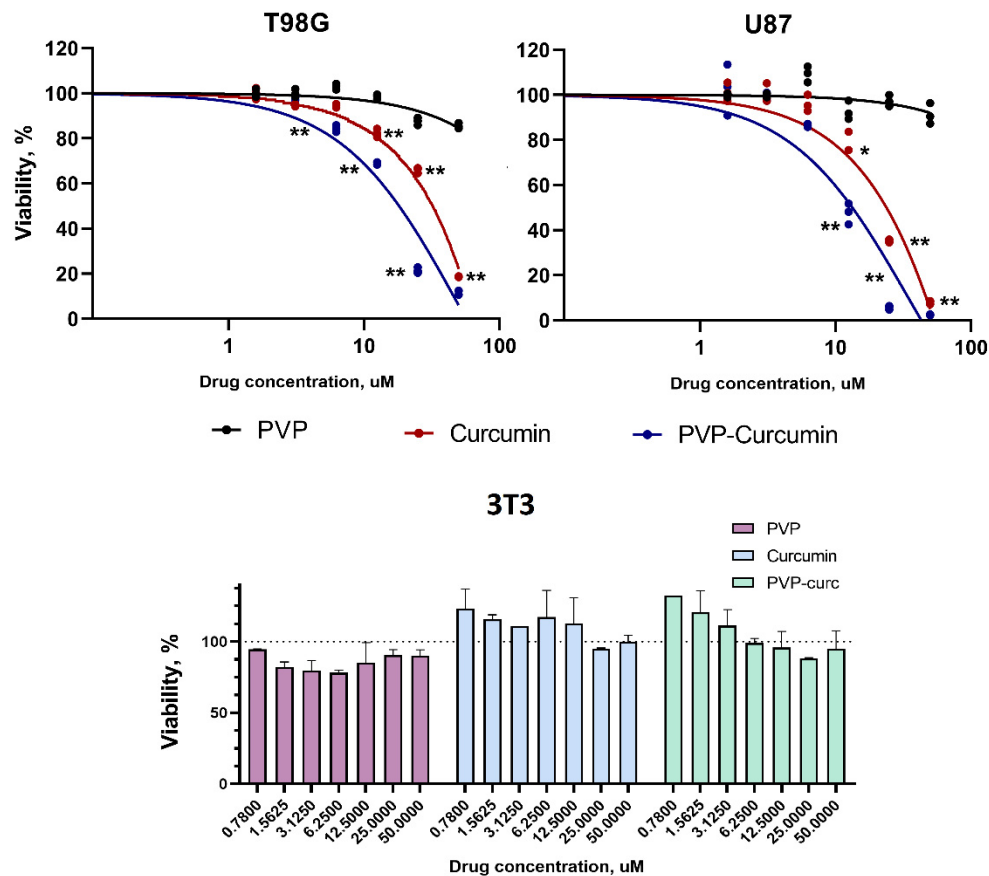


**Figure 3.** Cytotoxicity of PVP-Cur NPs, curcumin and PVP in T98G, U87 and 3T3 cells. The data were analysed using Graphpad Prism 6.01 software. Statistical analysis was held using ordinary one-way ANOVA followed by Dunnett's multiple comparisons test using Graphpad Prism 6.01 software (San Diego, CA, USA). \* $p < 0.05$  and \*\* $p < 0.005$  indicated significant difference from the control.

### 3.4. Cell uptake assay

PVP-Cur NPs were used for in vitro uptake studies in A431 epidermoid carcinoma and HEK293 human embryonic kidney cells. Relative fluorescence intensities were compared 60 minutes after cells were treated with nanoparticles and free curcumin. 60 minutes after treating cells with free curcumin and PVP-Cur NPs, it was shown that the relative fluorescence intensity of curcumin loaded into the nanoparticles was 1.5 times higher than that of the free curcumin (Figure 4). This difference in the absorption is due to the presence of an amphiphilic poly-N-vinylpyrrolidone shell and correlates with other studies related to curcumin encapsulation [53,54].

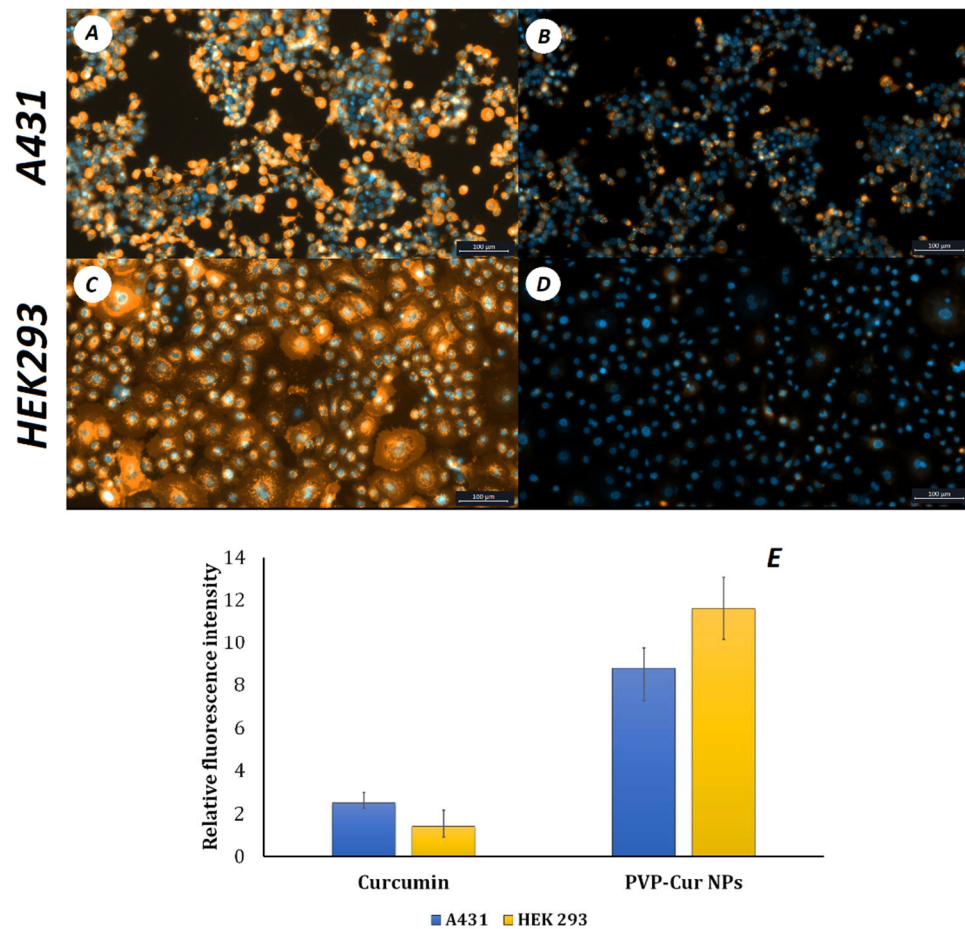


**Figure 4.** Uptake of curcumin-loaded nanocarriers (A&C) and free curcumin (B&D) by A431 and HEK 293 cells and relative fluorescence intensity after 60 minutes (E).

### 3.5. Fish Embryo Acute Toxicity Test (FET)

Zebrafish embryos treatment with PVP-Cur NPs in concentrations 25, 50 and 100  $\mu\text{M}$  provided neurotoxicity, that was characterized by increased motor activity of the tail (Figure 5).

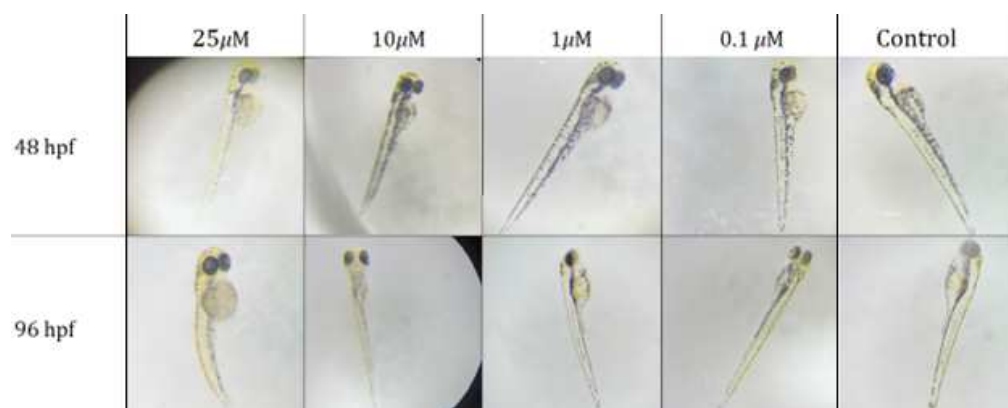


**Figure 5.** Danio rerio embryos aged 48 and 96 hpf after 24 h (48 hpf) and 72 h (96 hpf) of incubation with the studied curcumin nanoparticles at  $\times 40$  magnification.

The death of all embryos was observed after 24 hours of treatment with nanoparticles in concentrations of 50 and 100  $\mu\text{M}$  per loaded curcumin. Embryos that were treated with concentration 25  $\mu\text{M}$  had enlargement of the yolk sac and development delay after 24 hours, which persisted 72

hours after incubation/ 5 out of 6 embryos were found dead in 72 hours of experiments. Concentrations 10, 1 and 0.1  $\mu\text{M}$  provided no toxic effects. The  $\text{LC}_{50}$  value was determined as 23.7  $\mu\text{M}$  (Figure 6).

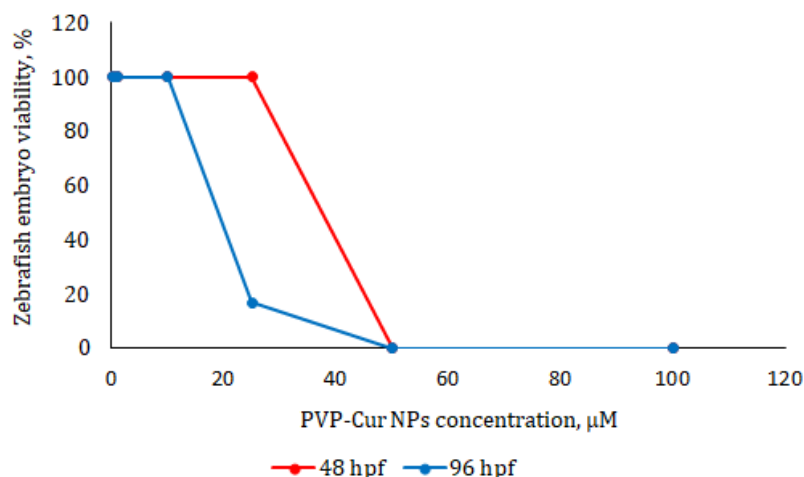


**Figure 6.** Survival of *Danio rerio* embryos (n=6 per group) during 24-h (48 hpf) and 72-h (96 hpf) incubation with curcumin-loaded poly(N-vinylpyrrolidone) nanoparticles PVP-Cur NPs. Lethal concentration  $\text{LC}_{50} = 23,7 \mu\text{M}$  (per curcumin contents) was determined by regression analysis using Graphpad Prism version 6.01.

#### 4. Discussion

We have previously shown the possibility of using amphiphilic PVPs with different molecular weights as a drug carriers. In this work, we show that amphiphilic poly(N-vinylpyrrolidone) may be a suitable curcumin carrier for cancer treatment.

Amphiphilic poly(N-vinylpyrrolidone) was synthesized by radical polymerization. The molecular weight of the resulting polymer was 6 kDa. As it was shown previously, this molecular weight accounts for suitable critical aggregation concentration and low toxicity of polymer [21,25,27]. PVP-Cur NPs were obtained by the solvent evaporation method: dispersion was carried out using an ultrasonic homogenizer using two infinitely compatible solvents (acetone-water). The samples obtained by this method have an average hydrodynamic diameter of about 200 nm as determined by DLS. It has been established that  $\zeta$ -potential ranges from -4 to -5 mV and differs little from the  $\zeta$ -potential of the outer cell membrane, which also has a close negative value and can range from -2 to -90 mV depending on the cell type, the composition of a particular membrane region and the pH of the environment [55,56]. It should be noted that the electrical stabilization of low-molecular-weight surfactants is reflected by high absolute surface charge values, while for high molecular weight surfactants (i.e., amphiphilic polymers), stabilization is achieved through different mechanisms (i.e., steric stabilization) and is not clearly reflected by the absolute value of the surface charge [57].

The mean diameter of the particles was  $118 \pm 40$  nm and  $127 \pm 41$  nm (mean  $\pm$  SD) according to TEM and AFM, respectively. The latter diameter was higher due to the AFM tip broadening. The height of the particles above the substrate ( $48 \pm 40$  nm) was far smaller than their lateral diameter, and the difference indicates intense flattening of the particles. Besides, it can be a consequence of the variations in the tip-sample interaction, which shift of the cantilever resonance frequency [58]. A similar difference between the height and width measured using AFM was previously observed for viruses [59,60], polymer nanoparticles [23], DNA [61], and other samples.

As curcumin is poorly water-soluble and dispersible substance, its encapsulation strategy using polymeric micelle-like nanoparticles was studied and revealed as a successful pass way to improve this essential physicochemical property.

The prepared NPs showed favorable long-term stability. This improvement could be explained by the unique core-shell structure of polymeric micelle-like aggregates immobilizing curcumin as

hydrophobic cargo in their hydrophobic inner core while the PVP hydrophilic shell contributes to solubilizing of these nanoparticles in the aqueous media.

In current study PVP-Cur NPs showed *in vitro* two-phase release profile in PBS (pH 7.4), composed of an immediate drug release followed by a sustained release. The two-phase delivery system helps in overcoming multiple dosing regimen problems. The initial burst release can be caused by the release of the drug entrapped in the polymeric shell of the nanoparticles, whereas the sustained release is the result of the drug diffusion from the hydrophobic core of the nanoparticles. Moreover, outer shell PVP layer probably forms a diffusion obstacle for the releasing drug, resulting in a slower release. Therefore, obtained results imply that the release profile of the studied nano-scaled carrier systems is significantly affected both by hydrophobic interactions in the nanoparticles core and by polymer coating layer.

*In vitro* curcumin release investigation in simulated gastric fluids with a sequence of pH values of 1.2, 6.8 and 7.4 revealed that low amount of curcumin release occurs at pH 1.2 and 6.8, while increased extent of sustained release is discovered at pH 7.4.

The release profile shows sustained slow, gradual release of curcumin at each point of time from polymeric nanoparticles at physiologic pH 7.4. Sustained drug release from the nanoparticles is an important feature, as it can dramatically increase the biologically active substance bioavailability and prolong diagnostic or therapeutic effect.

Curcumin obtains multiple effects *in vivo*, including antiproliferative, anti-inflammatory and antioxidant [62], which suggest that it can be utilized as a component of anticancer therapy. However, curcumin obtains poor stability *in vitro* and *in vivo* with a half-life of about 5 min, preventing it from exhibiting any therapeutically relevant effects [63]. Therefore, encapsulating curcumin into nanoparticles helps improve its bioavailability and ensures delivery to the lesion site where it can exert its therapeutic properties.

In the current study, cytotoxicity assays showed that PVP-Cur NPs are non-toxic for healthy fibroblasts. Previously, the low cytotoxicity of PVP NPs, including those with curcumin, was shown on different cell types including human embryonic stem cell derived fibroblasts (EBF-H9), human microvascular endothelial cells (HMEC-1), human embryonic kidney (HEK 293) and others [43,57,64–66].

Cell uptake assay showed that curcumin encapsulated in core/shell PVP-Cur NPs is transferred into the intracellular space 1.5 times more effectively than free curcumin. This difference in absorption is due to the presence of an amphiphilic poly-N-vinylpyrrolidone shell, which is similar to liposomes shell, and correlates with other studies related to curcumin encapsulation. Mechanism of action is similar to interaction of liposomes with cells. This is why the fluorescence of curcumin in cells is higher in the case of PVP-Cur NPs than in the case of free curcumin [67–69].

Due to accelerated cellular uptake of nanoparticles *in vitro*, the toxicity of PVP-Cur NPs increased compared to free curcumin against malignant cancer cells. This is consistent with the data previously obtained in [69]. Numerous studies demonstrate that curcumin can target signaling pathways involved in glioblastoma development: for example, by modulating the activity of transcription factors such as NF- $\kappa$ B and STAT3, and regulating the expression of genes implicated in malignant transformation and cell survival [71–73]. Curcumin is shown to modulate properties of glioblastoma stem cells via activation of autophagy [74]. Also, curcumin was reported to enhance the effect of radiation on glioma cells [75], making it a potential candidate for treatment of this type of cancer.

It can be assumed that such nanoparticles loaded with curcumin will be suitable for the treatment of malignant cancers, in particular glioblastoma. *In vivo* acute toxicity results on Zebrafish indicated that below a concentration of 23.7  $\mu$ M, PVP-Cur NPs are safe for use in living organisms.

## 5. Conclusion

Curcumin-loaded nanoparticles based on amphiphilic poly-N-vinylpyrrolidone were synthesized in this study. The molecular weight of PVP was 6 kDa, as the most suitable by its hydrophilic-hydrophobic balance. PVP-Cur NPs obtained by solvent evaporation method had



spherical form, average hydrodynamic diameter of about 200 nm and  $\zeta$ -potential was between -4 and -5 mV. PVP-Cur NPs are non-toxic for healthy fibroblast cells and very toxic for glioblastoma cells. The IC<sub>50</sub> of PVP-Cur NPs was determined to be 29.3±3.7  $\mu$ M and 20.7±1.3  $\mu$ M for T98G and U87 cells, respectively. In vivo experiments on Zebrafish shows that PVP-Cur NPs do not have acute toxicity at concentration below 23.7  $\mu$ M. The in vitro release profiles in different media indicate that amphiphilic PVP nanoparticles have prolonged release action and can be considered as prospective drug delivery system. Overall, the PVP-Cur NPs are promising for treatment of malignant cancers without toxic effect for healthy cells and organs.

**Author Contributions:** Conceptualization – A.K., A.L, Methodology – D.B., V.P., A.Y; Validation – A.Y., I.K; Formal analysis – D.D., M.G; Investigation, E.K., M.S. I.K., V.P.; Writing—original draft, A.L, A.K.; Writing—review & editing, D.B., M.G, A.Y., Visualization – M.S., A.K., A.L.; Project administration, A.K., D.D. All authors have read and agreed to the published version of the manuscript.

**Funding:** This work was financially supported by the Russian Science Foundation, grant No. 23-15-00468, <https://rscf.ru/project/23-15-00468/>.

**Institutional Review Board Statement:** The study was conducted in accordance with the European Convention for the Protection of Vertebrate Animals used for Experimental and other Scientific Purposes (CETS No. 123) and the protocol was approved by the Ethics Committee of N.N. Blokhin National Medical Research Centre for Oncology (Protocol 03p, 16 May 2023).

**Acknowledgments:** The TEM measurements were performed at the User Facilities Center «Electron microscopy in life sciences» at Lomonosov Moscow State University.

**Conflicts of Interest:** The authors declare no conflict of interest.

## References

1. D'souza, A. A.; Shegokar, R. Polyethylene glycol (PEG): a versatile polymer for pharmaceutical applications. *Expert Opin Drug Deliv*, **2016**, *13*, 1257-1275.
2. Suk, J. S.; Xu, Q.; Kim, N.; Hanes, J.; Ensign, L. M. PEGylation as a strategy for improving nanoparticle-based drug and gene delivery. *Adv Drug Deliv Rev*, **2016**, *99*, 28-51.
3. Shi, D.; Beasock, D.; Fessler, A.; Szebeni, J.; Ljubimova, J. Y.; Afonin, K. A.; Dobrovolskaia, M. A. To PEGylate or not to PEGylate: Immunological properties of nanomedicine's most popular component, polyethylene glycol and its alternatives. *Adv Drug Deliv Rev*, **2022**, *180*, 114079, 2022.
4. Tyler, B.; Gullotti, D.; Mangraviti, A.; Utsuki, T.; Brem, H. Polylactic acid (PLA) controlled delivery carriers for biomedical applications. *Adv Drug Deliv Rev*, **2016**, *15*, 163-175.
5. Casalini, T.; Rossi, F.; Castrovinci, A.; Perale, G. A Perspective on Polylactic Acid-Based Polymers Use for Nanoparticles Synthesis and Applications. *Front Bioeng Biotechnol*, **2019**, *7*, 259.
6. Na, Y.; Zhang, N.; Zhong, X.; Gu, J.; Yan, C.; Yin, S.; Lei, X.; Zhao, J.; Geng, F. Polylactic-co-glycolic acid-based nanoparticles modified with peptides and other linkers cross the blood-brain barrier for targeted drug delivery. *Nanomedicine (Lond)*, **2023**, *18*, 125-143.
7. Rocha, C. V.; Gonçalves, V.; da Silva, M. C.; Bañobre-López, M.; Gallo, J. PLGA-Based Composites for Various Biomedical Applications. *Int J Mol Sci*, **2022**, *23*, 2034.
8. Liu, C.; Zhang, S.; McClements, D. J.; Wang, D.; Xu, Y. Design of Astaxanthin-Loaded Core-Shell Nanoparticles Consisting of Chitosan Oligosaccharides and Poly(lactic-co-glycolic acid): Enhancement of Water Solubility, Stability, and Bioavailability. *J Agric Food Chem*, **2019**, *67*, 5113-5121.
9. Mohammadian, S.; Khazaei, M.; Maghami, P.; Avan, A.; Rezaei, M. Polycaprolactone-based Nanocarriers Containing 5-fluorouracil as a Therapeutic Guided Drug Delivery Approach for Enhancing Anticancer Activity. *Curr Cancer Drug Targets*, **2023**, *23*, 524-533.
10. Pohlmann, A. R.; Fonseca, N. F.; Paese, K.; Detoni, C. B.; Coradini, K.; Beck, R. C.; Guterres, S. S. Poly( $\epsilon$ -caprolactone) microcapsules and nanocapsules in drug delivery. *Expert Opin Drug Deliv*, **2013**, *10*, 623-638.
11. Franco, P.; De Marco, I. The Use of Poly(N-vinyl pyrrolidone) in the Delivery of Drugs: A Review. *Polymers*, **2020**, *12*, 1114.
12. Waleka, E.; Stojek, Z.; Karbarz, M. Activity of Povidone in Recent Biomedical Applications with Emphasis on Micro- and Nano Drug Delivery Systems. *Pharmaceutics*, **2021**, *13*, 654.

13. Luo, Y.; Hong, Y.; Shen, L.; Wu, F.; Lin, X. Multifunctional Role of Polyvinylpyrrolidone in Pharmaceutical Formulations. *AAPS PharmSciTech*, **2021**, *22*, 34.
14. Moffitt, E. A. Blood substitutes. *Can Anaesth Soc J*, **1975**, *22*, 12-19.
15. Bigliardi, P. L.; Alsagoff, S. A. L.; El-Kafrawi, H. Y.; Pyon, J.-K.; Wa, C. T. C.; Villa, M. A. Povidone iodine in wound healing: A review of current concepts and practices. *Int J Surg*, **2017**, *44*, 260-268.
16. Malet, F.; Karsenti, D.; Pouliquen, P. Preservative-free ocular hydrating agents in symptomatic contact lens wearers: saline versus PVP solution. *Eye Contact Lens*, **2003**, *29*, 38-43.
17. Inactive Ingredient Search for Approved Drug Products. Available: <https://www.accessdata.fda.gov/scripts/cder/iig/index.cfm>.
18. Kulikov, P. P.; Luss, A. L.; Nelemans, L. C.; Shtilman, M. I.; Mezhuev, Y. O.; Kuznetsov, I. A.; Sizova, O. Y.; Christiansen, G.; Pennisi, C. P.; Gurevich, L. Synthesis, Self-Assembly and In Vitro Cellular Uptake Kinetics of Nanosized Drug Carriers Based on Aggregates of Amphiphilic Oligomers of N-Vinyl-2-pyrrolidone. *Materials*, **2021**, *14*, 20.
19. Kuskov, A. N.; Kulikov, P. P.; Goryachaya, A. V.; Tzatzarakis, M. N.; Docea, A. O.; Velonia, K.; Shtilman, M. I.; Tsatsakis, A. M. Amphiphilic poly-N-vinylpyrrolidone nanoparticles as carriers for non-steroidal, anti-inflammatory drugs: In vitro cytotoxicity and in vivo acute toxicity study. *Nanomedicine*, **2017**, *13*, 1021-1030.
20. Kuskov, A. N.; Voskresenskaya, A. A.; Goryachaya, A. V.; Shtilman, M. I.; Spandidos, D. A.; Rizos, A. K.; Tsatsakis, A. M. Amphiphilic poly-N-vinylpyrrolidone nanoparticles as carriers for non-steroidal anti-inflammatory drugs: Characterization and in vitro controlled release of indomethacin. *Int J Mol Med*, **2010**, *26*, 85-94.
21. Kuskov, A.; Nikitovich, D.; Berdiaki, A.; Shtilman, M.; Tsatsakis, A. Amphiphilic Poly-N-vinylpyrrolidone Nanoparticles as Carriers for Nonsteroidal, Anti-Inflammatory Drugs: Pharmacokinetic, Anti-Inflammatory, and Ulcerogenic Activity Study. *Pharmaceutics*, **2022**, *14*, 925.
22. Artyukhov, A. A.; Nechaeva, A. M.; Shtilman, M. I.; Chistyakov, E. M.; Svistunova, A. Y.; Bagrov, D. V.; Kuskov, A. N.; Docea, A. O.; Tsatsakis, A. M.; Gurevich, L.; Mezhuev, Y. O. Nanoaggregates of Biphilic Carboxyl-Containing Copolymers as Carriers for Ionically Bound Doxorubicin. *Materials*, **2022**, *15*, 7136.
23. Yamskov, I. A.; Kuskov, A. N.; Babievsky, K. K.; Berezin, B. B.; Krayukhina, M. A.; Samoylova, N. A.; Tikhonov, V. E.; Shtilman, M. I. Novel liposomal forms of antifungal antibiotics modified by amphiphilic polymers. *Appl Biochem Microbiol*, **2008**, *44*, 624-628.
24. Yagolovich, A.; Kuskov, A.; Kulikov, P.; Kurbanova, L.; Bagrov, D.; Artykov, A.; Gasparian, M.; Sizova, S.; Oleinikov, V.; Gileva, A.; Kirpichnikov, M.; Dolgikh, D.; Markvicheva, E. Amphiphilic Poly(N-vinylpyrrolidone) Nanoparticles Conjugated with DR5-Specific Antitumor Cytokine DR5-B for Targeted Delivery to Cancer Cells. *Pharmaceutics*, **2021**, *13*, 1413.
25. Yagolovich, A.; Kuskov, A.; Kulikov, P.; Kurbanova, L.; Gileva, A.; Markvicheva, E. Antitumor Cytokine DR5-B-Conjugated Polymeric Poly(N-vinylpyrrolidone) Nanoparticles with Enhanced Cytotoxicity in Human Colon Carcinoma 3D Cell Spheroids. *Mat Proceed*, **2021**, *7*, 8.
26. Kuskov, A.; Selina, O.; Kulikov, P.; Imatdinov, I.; Balysheva, V.; Kryukov, A.; Shtilman, M.; Markvicheva, E. Amphiphilic Poly(N-Vinylpyrrolidone) Nanoparticles Loaded with DNA Plasmids Encoding Gn and Gc Glycoproteins of the Rift Valley Fever Virus: Preparation and In Vivo Evaluation. *CS Appl. Bio Mater.*, **2021**, *4*, 6084-6092.
27. Luss, A. L.; Kulikov, P. P.; Romme, S. B.; Andersen, C. L.; Pennisi, C. P.; Docea, A. O.; Kuskov, A. N.; Velonia, K.; Mezhuev, Y. O.; Shtilman, M. I.; Tsatsakis, A. M.; Gurevich, L. Nanosized carriers based on amphiphilic poly-N-vinyl-2-pyrrolidone for intranuclear drug delivery. *Nanomedicine*, **2018**, *13*, 703-715.
28. Ganji, A.; Farahani, I.; Saedifar, A. M.; Mosayebi, G.; Ghazavi, A.; Majeed, M.; Jamialahmadi, T.; Sahebkar, A. Protective Effects of Curcumin against Lipopolysaccharide-Induced Toxicity. *Curr Med Chem*, **2021**, *28*, 6915-6930.
29. Barua, N.; Buragohain, A. K. Therapeutic Potential of Curcumin as an Antimycobacterial Agent. *Biomolecules*, **2021**, *11*, 1278.
30. Tomeh, M. A.; Hidianamrei, R.; Zhao, X. A Review of Curcumin and Its Derivatives as Anticancer Agents. *Int J Mol Sci*, **2019**, *20*, 1033.
31. Feltrina, F. d. S.; Agner, T.; Sayer, C.; Lona, L. M. F. Curcumin encapsulation in functional PLGA nanoparticles: A promising strategy for cancer therapies. *Adv Colloid Interface Sci*, **2022**, *300*, 102582.

32. Ataei, M.; Gumprich, E.; Kesharwani, P.; Jamialahmadi T.; Sahebkar, A. Recent advances in curcumin-based nanoformulations in diabetes. *J Drug Target*, **2023**, *31*, 671-684.
33. Hartogh, D. J. D.; Gabriel, A.; Tsiani, E. Antidiabetic Properties of Curcumin I: Evidence from In Vitro Studies. *Nutrients*, **2020**, *12*, 118.
34. Chamani, S.; Moossavi, M.; Naghizadeh, A.; Abbasifard, M.; Majeed, M.; Johnston T. P.; Sahebkar, A. Immunomodulatory effects of curcumin in systemic autoimmune diseases. *Phytother Res*, **2022**, *36*, 1616-1632.
35. Fridlender, M.; Kapulnik, Y.; Koltai, H. Plant derived substances with anti-cancer activity: from folklore to practice. *Front Plant Sci*. **2015**; *6*, 799.
36. Iqbal, J.; Abbasi, B.A.; Mahmood, T.; Kanwal, S.; Ali, B.; Shah, S.A.; Khalil, A.T. Plant-derived anticancer agents: A green anticancer approach. *Asian Pac J Trop Biomed*. **2017**, *7*, 1129-1150.
37. de Waure, C.; Bertola, C.; Baccarini, G.; Chiavarini, M.; Mancuso, C. Exploring the Contribution of Curcumin to Cancer Therapy: A Systematic Review of Randomized Controlled Trials. *Pharmaceutics*, **2023**, *15*, 1275.
38. Omidian, H.; Wilson, R.L.; Chowdhury, S.D. Enhancing Therapeutic Efficacy of Curcumin: Advances in Delivery Systems and Clinical Applications. *Gels*, **2023**, *9*, 596.
39. Banazadeh, M.; Behnam, B.; Ganjooei, N.A.; Gowda, B.H.J.; Kesharwani, P.; Sahebkar, A. Curcumin-based nanomedicines: A promising avenue for brain neoplasm therapy. *J Drug Deliv Sci Technol*, **2023**, *89*, 105040.
40. Anand, P.; Kunnumakkara, A. B.; Newman, R. A.; Aggarwal, B. B. Bioavailability of curcumin: problems and promises. *Mol Pharm*, **2007**, *4*, 807-818.
41. Sanidad, K. Z.; Sukamtoh, E.; Xiao, H.; McClements, D. J.; Zhang, G. Curcumin: Recent Advances in the Development of Strategies to Improve Oral Bioavailability. *Annu Rev Food Sci Technol*, **2019**, *10*, 597-617.
42. Liu, C.; Yuan, Y.; Ma, M.; Zhang, S.; Wang, S.; Li, Y.; Xu, H.; Wang, D. Self-assembled composite nanoparticles based on zein as delivery vehicles of curcumin: role of chondroitin sulfate. *Food Funct*, **2020**, *11*, 5377-5388.
43. Berdiaki, A.; Perisynaki, E.; Stratidakis, A.; Kulikov, P. P.; Kuskov, A. N.; Stivaktakis, P.; Henrich-Noak, P.; Luss, A. L.; Shtilman, M. I.; Tzanakakis, G. N.; Tsatsakis, A.; Nikitovich, D. Assessment of Amphiphilic Poly-N-vinylpyrrolidone Nanoparticles' Biocompatibility with Endothelial Cells in Vitro and Delivery of an Anti-Inflammatory Drug. *Mol Pharm*, **2020**, *17*, 4212-4225.
44. Estifeeva, T. M.; Barmin, R. A.; Rudakovskaya, P. G.; Nechaeva, A. M.; Luss, A. L.; Mezhuev, Y. O.; Chernyshev, V. S.; Krivoborodov, E. G.; Klimenko, O. A.; Sindeeva, O. A.; Demina, P. A.; Petrov, K. S.; Chuprov-Netochin, R. N.; Fedotkina, E. P.; Korotchenko, O. E.; Sencha, E. A.; Sencha, A. N.; Shtilman, M. I.; Gorin, D. A. Hybrid (Bovine Serum Albumin)/Poly(N-vinyl-2-pyrrolidone-co-acrylic acid)-Shelled Microbubbles as Advanced Ultrasound Contrast Agents. *ACS Appl Bio Mater*, **2022**, *5*, 3338-3348.
45. Schneider, C. A.; Rasband, W. S.; Eliceiri, K. W. NIH Image to ImageJ: 25 years of image analysis. *Nat Methods*, **2012**, *9*, 671-675.
46. Yaminsky, I.; Akhmetova, A.; Meshkov, G. Femtoscan online software and visualization of nano-objects in high-resolution microscopy. *NanoIndustry*, **2018**, *11*, 44-48.
47. Ranjan, A.P.; Mukerjee, A.; Helson, L.; Vishwanatha, J.K. Scale up, optimization and stability analysis of Curcumin C3 complex-loaded nanoparticles for cancer therapy. *J Nanobiotechnology*, **2012**, *10*, 38.
48. Hasan, M.; Latifi, S.; Kahn, C.; Tamayol, A.; Habibey, R.; Passeri, E.; Linder, M.; Arab-Tehrany, E. The Positive Role of Curcumin-Loaded Salmon Nanoliposomes on the Culture of Primary Cortical Neurons. *Mar Drugs*, **2018**, *16*, 218.
49. Hasan, M.; Elkhoury, K.; Kahn, C.; Arab-Tehrany, E.; Linder, M. Preparation, Characterization, and Release Kinetics of Chitosan-Coated Nanoliposomes Encapsulating Curcumin in Simulated Environments. *Molecules*, **2019**, *24*, 2023.
50. von Hellfeld, R.; Brotzmann, K.; Baumann, L.; Strecker, R.; Braunbeck, T. Adverse effects in the fish embryo acute toxicity (FET) test: a catalogue of unspecific morphological changes versus more specific effects in zebrafish (*Danio rerio*) embryos. *Environ Sci Eur*, **2020**, *32*, 122.
51. Bagrov, D. V.; Adlerberg, V. V.; Skryabin, G. O.; Nikishin, I. I.; Galetsky, S. A.; Tchevkina, E. M.; Kirpichnikov, M. P.; Shaitan, K. V. AFM-TEM correlation microscopy and its application to lipid nanoparticles. *Microsc Res Tech*, **2023**, *86*, 781-790.

52. Ito, T.; Sun, L.; Bevan, M. A.; Crooks, R. M. Comparison of nanoparticle size and electrophoretic mobility measurements using a carbon-nanotube-based coulter counter, dynamic light scattering, transmission electron microscopy, and phase analysis light scattering. *Langmuir*, **2004**, *20*, 6940-6945.
53. Liu, Z.; Lansley, A. B.; Duong, T. N.; John, D. S.; Pannala, A. S. Increasing Cellular Uptake and Permeation of Curcumin Using a Novel Polymer-Surfactant Formulation. *Biomolecules*, **2022**, *12*, 1739.
54. Huang, L.; Cai, M.; Xie, X.; Chen, Y.; Luo, X. Uptake enhancement of curcumin encapsulated into phosphatidylcholine-shielding micelles by cancer cells. *J Biomater Sci Polym Ed*, **2014**, *25*, 1407-1424.
55. Loufakis, D. N.; Cao, Z.; Ma, S.; Mittelman, D.; Lu, C. Focusing of mammalian cells under an ultrahigh pH gradient created by unidirectional electropulsation in a confined microchamber. *Chem Sci*, **2014**, *5*, 3331.
56. Metwally, S.; Stachewicz, U. Surface potential and charges impact on cell responses on biomaterials interfaces for medical applications. *Mater Sci Eng C Mater Biol Appl*, **2019**, *104*, 109883.
57. Kuskov, A.N.; Kulikov, P.P.; Goryachaya, A.V.; Tzatzarakis, M.N.; Tsatsakis, A.M.; Velonia, K.; Shtilman, M.I. Self-assembled amphiphilic poly-N-vinylpyrrolidone nanoparticles as carriers for hydrophobic drugs: Stability aspects. *J Appl Polym Sci*. **2017**, *135*, 45637.
58. Ebenstein, Y.; Nahum, E.; Banin, U. Tapping Mode Atomic Force Microscopy for Nanoparticle Sizing: Tip-Sample Interaction Effects. *Nano Letters*, **2002**, *2*, 945-950.
59. Moiseenko, A. V.; Bagrov, D. V.; Vorovitch, M. F.; Uvarova, V. I.; Veselov, M. M.; Kashchenko, A. V.; Ivanova, A. L.; Osolodkin, D. I.; Egorov, A. M.; Ishmukhametov, A. A.; Shaitan, K. V.; Sokolova, O. S. Size Distribution of Inactivated Tick-Borne Encephalitis Virus Particles Revealed by a Comprehensive Physicochemical Approach. *Biomedicines*, **2022**, *10*, 2478.
60. Bagrov, D. V.; Glukhov, G. S.; Moiseenko, A. V.; Karlova, M. G.; Litvinov, D. S.; Zaitsev, P. A.; Kozlovskaya, L. I.; Shishova, A. A.; Kovpak, A. A.; Ivin, Y. Y.; Piniaeva, A. N.; Oksanich, A. S.; Volo, V. P.; Osolodkin, D. I.; Ishmukhametov, A. A.; Egorov, A. M.; Shaitan, K. V.; Kirpichnikov, M. P.; Sokolova, O. S. Structural characterization of  $\beta$ -propiolactone inactivated severe acute respiratory syndrome coronavirus 2 (SARS-CoV-2) particles. *Microsc Res Tech*, **2022**, *85*, 562-569.
61. Klinov, D. V.; Dubrovina, E. V.; Yaminsky, I. V. Scanning Probe Microscopy of DNA on Mica and Graphite. *AIP Conf. Proc.*, **2003**, *696*, 452-456.
62. Labanca, F.; Ullah, H.; Khan, H.; Milella, L.; Xiao, J.; Dajic-Stevanovic Z.; Jeandet P. Therapeutic and Mechanistic Effects of Curcumin in Huntington's Disease. *Curr Neuropharmacol*, **2021**, *19*, 1007-1018.
63. Persano, F.; Gigli, G.; Leporatti S. Natural Compounds as Promising Adjuvant Agents in The Treatment of Gliomas. *Int. J. Mol. Sci.* **2022**, *23*, 3360.
64. Wei, H.; Jiang, D.; Yu, B.; Ni, D.; Li, M.; Long, Y.; Ellison, P.A.; Siamof, C.M.; et. al. Nanostructured polyvinylpyrrolidone-curcumin conjugates allowed for kidney-targeted treatment of cisplatin induced acute kidney injury. *Bioact Mater.* **2023**, *19*, 282-291.
65. Tsatsakis, A.; Stratidakis, A.K.; Goryachaya, A.V.; Tzatzarakis, M.N.; Stivaktakis, P.D.; Docea, A.O.; Berdiaki, A.; Nikitovich, D.; et.al. In vitro blood compatibility and in vitro cytotoxicity of amphiphilic poly-N-vinylpyrrolidone nanoparticles. *Food Chem Toxicol.* **2019**, *127*, 42-52.
66. Kuskov, A.N.; Kulikov, P.P.; Shtilman, M.I.; Rakitskii, V.N.; Tsatsakis, A.M. Amphiphilic poly-N-vinylpyrrolidone nanoparticles: Cytotoxicity and acute toxicity study. *Food Chem Toxicol.* **2016**, *96*, 273-279.
67. Gholami, L.; Momtazi-Borojeni, A.A.; Malaekhe-Nikouei, B.; Nikfar, B.; Amanolahi, F.; Mohammadi, A.; Oskuee, R.K. Selective Cellular Uptake and Cytotoxicity of Curcumin-encapsulated SPC and HSPC Liposome Nanoparticles on Human Bladder Cancer Cells. *Curr Pharm Des*, **2023**, *29*, 1046-1058.
68. Bolger, G.T.; Licollari, A.; Bagshaw, R.; Tan, A.; Greil, R.; Vcelar, B.; Majeed, M.; Sordillo, P. Intense Uptake of Liposomal Curcumin by Multiple Myeloma Cell Lines: Comparison to Normal Lymphocytes, Red Blood Cells and Chronic Lymphocytic Leukemia Cells. *Anticancer Res*, **2019**, *39*, 1161-1168.
69. Apiratikul, N.; Penglong, T.; Suksen, K.; Svasti, S.; Chairoungdua, A.; Yingyongnarongkul B. In vitro Delivery of Curcumin with Cholesterol-Based Cationic Liposomes. *Russ J Bioorg Chem*, **2013**, *39*, 444-450.
70. Bi, C.; Miao, X.Q.; Chow, S.F.; Wu, W.J.; Yan, R.; Liao, Y.H.; Chow, A. H.-L.; Zheng, Y. Particle size effect of curcumin nanosuspensions on cytotoxicity, cellular internalization, in vivo pharmacokinetics and biodistribution. *Nanomedicine* **2017**, *13*, 943-953.
71. Hesari, A.; Rezaei, M.; Rezaei, M.; Dashtianhangar, M.; Fathi, M.; Rad, J.G.; Momeni, F.; Avan, A.; Ghasemi, F. Effect of curcumin on glioblastoma cells. *J. Cell Physiol.* **2019**, *234*, 10281-10288.

72. Weissenberger, J.; Priester, M.; Bernreuther, C.; Rakel, S.; Glatzel, M.; Seifert, V.; Kögel, D. Dietary curcumin attenuates glioma growth in a syngeneic mouse model by inhibition of the JAK1,2/STAT3 signaling pathway. *Clin Cancer Res.* **2010**, *16*, 5781-5795.
73. Shahcheraghi, S.H.; Zangui, M.; Lotfi, M.; Ghayour-Mobarhan, M.; Ghorbani, A.; Jaliani, H. Z.; Sadeghnia, H.R.; Sahebkar, A. Therapeutic Potential of Curcumin in the Treatment of Glioblastoma Multiforme. *Curr. Pharm. Des.* **2019**, *25*, 333-342.
74. Ryskalin, L.; Biagioni, F.; Busceti, C.L.; Lazzeri, G.; Frati, A.; Fornai, F. The Multi-Faceted Effect of Curcumin in Glioblastoma from Rescuing Cell Clearance to Autophagy-Independent Effects. *Molecules* **2020**, *25*, 4839.
75. Zoi, V.; Galani, V.; Vartholomatos, E.; Zacharopoulou, N.; Tsoumeleka, E.; Gkizas, G.; Bozios, G.; Tsekeris, P.; Chousidis, I.; Leonardos, I.; et.al. Curcumin and Radiotherapy Exert Synergistic Anti-Glioma Effect In Vitro. *Biomedicines* **2021**, *9*, 1562.

**Disclaimer/Publisher's Note:** The statements, opinions and data contained in all publications are solely those of the individual author(s) and contributor(s) and not of MDPI and/or the editor(s). MDPI and/or the editor(s) disclaim responsibility for any injury to people or property resulting from any ideas, methods, instructions or products referred to in the content.